In vitro evaluation of gelatin and chitosan electrospun fibers as artificial guide in peripheral nerve repair: a comparative study

In vitro evaluation of gelatin and chitosan electrospun fibers as artificial guide in peripheral nerve repair: a comparative study.

Gnavi S. [a,b]*, Fornasari B.E.[a,b], Tonda-Turo C.[c], Laurano R. [c], Zanetti M.[d], Ciardelli G.[c,e] and Geuna S.[a,b]

a Department of Clinical and Biological Sciences, University of Torino, Orbassano, 10043, Italy; stefano.geuna@unito.it

b Neuroscience Institute of the Cavalieri-Ottolenghi Foundation, University of Torino, Orbassano, 10043, Italy; sara.gnavi@unito.it; benedettaelena.fornasari@unito.it; stefano.geuna@unito.it

c Politecnico di Torino, Department of Mechanical and Aerospace Engineering, Politecnico of Torino, Torino, 10100 Italy; chiara.tondaturo@polito.it

d Nanostructured Interfaces and Surfaces, Department of Chemistry, University of Torino, Torino, 10100 Italy; marco.zanetti@unito.it

e CNR-IPCF UOS, Pisa, 56124, Italy; gianluca.ciardelli@polito.it

*Corresponding author:

Gnavi Sara, PhD

University of Turin, Department of Clinical and Biological Sciences and Neuroscience Institute of the Cavalieri-Ottolenghi Foundation

Regione Gonzole 10, 10043 - Orbassano (TO) – ITALY

tel (+39) 011.670.5433/36

fax (+39) 011.903.8639

e-mail: sara.gnavi@unito.it

Keywords: chitosan, gelatin, electrospun fibers, peripheral nerve repair, biomimetic materials, aligned fibers, random fibers

This article has been accepted for publication and undergone full peer review but has not been through the copyediting, typesetting, pagination and proofreading process which may lead to differences between this version and the Version of Record. Please cite this article as doi: 10.1002/term.2351

Abstract

Random and aligned gelatin and chitosan nano-fibers have been prepared by electrospinning tuning the collector rotation speed. The effect of fiber alignment on cell adhesion and proliferation was assessed *in vitro* by using different Schwann cell and neuronal models. Moreover, actin cytoskeleton organization, lamellipodia and filipodia formation and axon outgrowth were evaluated. Gelatin and chitosan fibers induced similar adhesion and proliferation rate. Gelatin and chitosan random fibers promoted higher adhesion and proliferation rate induction in comparisons to the aligned ones. Although, gelatin and chitosan fibers alignment resulted in SC and axon oriented growth. Filipodia formation was higher on aligned fibers, suggesting that these substrates can promote higher cell migration in comparison to random ones. 50B11 (neuronal cell line) differentiation was higher on gelatin fibers, whereas no differences were observed in DRG explants model. These data suggest that both gelatin and chitosan fibers can be promising substrates to be used in peripheral nerve reconstruction.

1. INTRODUCTION

In recent years, the research for effective biomimetic materials for peripheral nerve reconstruction has generated interest in the use of engineered electrospun fibers as alternatives to autografts (Ichihara, Inada et al. 2008; Siemionow and Brzezicki 2009; Biazar, Khorasani et al. 2010; Gu, Ding et al. 2011). Electrospun fiber can be used as internal filler for hollow nerve guide. Electrospun random or align fibers can be easily prepared by electrospinning technique (Bhardwaj and Kundu 2010). In the electrospinning technique, a polymer solution is forced into a capillary tube and subjected to an electric field. When the applied electric field reaches a critical value, the repulsive electrical forces overcome the surface tension forces and, a charged jet of the solution is ejected from the capillary tip (Yarin, Koombhongse et al. 2001; Adomaviciute and Milasius 2007; Christopherson, Song et al. 2009). Then, an unstable jet occurs in the gap between the Taylor cone and the collector,

which leads to solvent and polymer fiber formation (Yarin, Koombhongse et al. 2001; Adomaviciute and Milasius 2007; Christopherson, Song et al. 2009). Particularly, random fibers are collected on a fixed collector, whereas the orientation of nano-fibers along a preferred direction can be obtained by using a rapidly rotating cylindrical collector (Yarin, Koombhongse et al. 2001; Adomaviciute and Milasius 2007; Christopherson, Song et al. 2009). Moreover, fibers diameter can range from nano-meter to micro-meter size depending on different parameters such as polymer concentration and solution flow rate (Yarin, Koombhongse et al. 2001; Adomaviciute and Milasius 2007; Christopherson, Song et al. 2009). Fibers alignment is of interest for tissue engineering purposes in order to give to the cells a preferred growth direction. Several materials, both synthetic and natural, have been used in the preparation of electrospun fibers.

In the past years, many synthetic biodegradable polymers, polyglycolic acid (PGA) and polylactic acid (PLA) or polyhydroxybutyrate, and synthetic nonabsorbable materials, such as silicone have been used as artificial nerve guide (Dahlin, Anagnostaki et al. 2001; Biazar, Khorasani et al. 2010). Food and Drug Administration (FDA) and European Commission (EC) approved a number of synthetic (biodegradable and not degradable) and natural materials, among them Neurotube™, Neura-Gen™ and Neurolac tubes made of poly(glycolide) (PGA), collagen and poly(dl-lactide-ε-caprolactone), respectively. These materials resulted in poor nerve repair and functional recovery in comparison to autograft (Daly, Yao et al. 2012). Silicone nerve conduits have been clinically used providing mechanical support for peripheral nerve regeneration although these conduits are not degradable and cannot be absorbed *in vivo* (de Ruiter, Malessy et al. 2009; Carriel, Alaminos et al. 2014). Nerve conduits made of polyesters such as polylactic acid (PLA), poly-e-caprolactone (PCL) and

polyglicolic acid (PGA) have been used in nerve gaps repair (Deumens, Bozkurt et al. 2010; Carriel, Alaminos et al. 2014). PCL nerve conduits have been widely used, although there are few clinical reports about its use in nerve reconstruction probably because of physical damage caused by this kind of conduit. PGA-based nerve conduits have excellent mechanical properties however, they progressively lose their strength. Moreover, PGA hydrolysis decreases the pH that cannot be neutralized by the cellular microenviroment resulting in tissue inflammation and necrosis (Carriel, Alaminos et al. 2014). On the other hand, natural materials such as collagen, fibrin, glycoproteins and proteglycans are highly biocompatible and biodegradable (Siemionow and Brzezicki 2009; Deumens, Bozkurt et al. 2010; Rahmany and Van Dyke 2013; Carriel, Alaminos et al. 2014).

During the last years, in order to overcome the disadvantages of artificial materials, gelatin and chitosan scaffolds have been used as alternative to synthetic polymers because of their biomimetic properties (Gnavi, Barwig et al. 2013).

Biomimetic materials to be used in nerve reconstruction should reduce immunogenicity and inflammatory reactions, be biodegradable, support surgical manipulation, prevent collapse, display a certain degree of porosity to promote efficient exchange of nutrients and waste, and provide topological signalling to cells in order to facilitate reorganization of the inner configuration of the nerve (Ciardelli and Chiono 2006; Chiono, Tonda-Turo et al. 2009; Zhang, Quigley et al. 2014). In recent years a number of study demonstrated that gelatin and chitosan are promising biomimetic materials (Ciardelli and Chiono 2006; Gnavi, Barwig et al. 2013). Gelatin is a natural polymer obtained from the thermal denaturation of collagen. In comparison to collagen, gelatin is biocompatible, biodegradable, does not provoke immune-rejection reactions, and maintains molecular cues that regulate cell

behaviour (Ciardelli and Chiono 2006). However, gelatin can be dissolved in water and the rapid degradation rate of gelatin can be the limiting factor of using gelatin in wound healing. Nevertheless, the degradation can be reduced by using crosslinking agents such as γ-glycidoxypropyltrimethoxysilane (GPTMS) or genipin, thus avoiding the use of acidic solutions and potentially cytotoxic solvents (Zhang, Huang et al. 2009; Tonda-Turo, Cipriani et al. 2013; Gnavi, Fornasari et al. 2015). Chitosan is derived from chitin by performing alkaline hydrolysis of acetamide groups. In order to obtain chitosan a combination of high temperature (100°C) with strong aqueous alkali treatments are used to deacetylate chitin (Khor and Lim 2003; Gnavi, Barwig et al. 2013). The major limitations in the employ of chitosan in biomedical applications are its low solubility at neutral pH and high viscosity (Khor and Lim 2003; Gnavi, Barwig et al. 2013). Despite these disadvantages, chitosan has positive properties such as biocompatibility, biodegradability, and no toxicity that make this polymer suitable in biomedical field (Khor and Lim 2003; Gnavi, Barwig et al. 2013). Several chitosan products have been approved by the Food and Drug Administration (FDA). Moreover, chitosan has been used to produce laser activated film surgical adhesive (SurgiLux) that can be used as an alternative to microsurgery for peripheral nerve repair (Foster and Karsten 2012).

As previously mentioned, despite biocompatibility and biochemical composition, other parameters must be taken in account in innovative inner filler development. Particularly, the topography (three-dimensional architecture) of the inner filler influences cell organization of the regenerating tissue (Agarwal 2008; Bacakova, Filova et al. 2011; Harvey, Hill et al. 2013). The properties of an internal filler such as fiber composition, diameter and orientation can be diversified to modulate Schwann cell (SC) and axon growth (Agarwal 2008; Bacakova,

Filova et al. 2011; Harvey, Hill et al. 2013). A number of studies have reported that topography plays an important role in controlling adhesion, proliferation, survival and migration of different cell types by affecting formation and distribution of focal adhesion plaques, actin cytoskeleton reorganization and/or lamellipodium and filopodia formation (Agarwal 2008; Bacakova, Filova et al. 2011; Gnavi, Barwig et al. 2013; Harvey, Hill et al. 2013; Tonda-Turo, Cipriani et al. 2013; Gnavi, Fornasari et al. 2015).

In this study we developed nano-fibrous matrices, made up of gelatin or chitosan, characterized by different fibers orientation (random or aligned). RT4-D6P2T schwannoma cell line, primary SC and dorsal root ganglia (DRG) neuronal 50B11 cell line cultures and DRG explants have been set up to perform the experiments. Gelatin and chitosan fibers of 300 nm size were prepared and *in vitro* and *ex vivo* studies were performed to investigate whether the topography and polymer composition modulate SC adhesion, survival and proliferation and neurite outgrowth.

2. MATERIAL AND METHODS

2.1 Gelatin and chitosan fibers preparation

Medical grade chitosan (CS) (molecular weight 200 – 400 kDa, deacetylation degree ≥ 92.6 %) was purchased by Kraeber GmbH & Co. PEO (Mw 900.000 Da), gelatin (type A from porcine skin), (3-Glycidoxypropyl)methyldiethoxysilane (GPTMS) and polyethylene oxide (PEO), dibasic sodium phosphate (DSP), dimethyl sulfoxide (DMSO) and solvents were supplied from Sigma Aldrich.

Crosslinked gelatin (GL) nano-fibers were prepared as previously described by author (Tonda-Turo, Cipriani et al. 2013; Gnavi, Fornasari et al. 2015; Gnavi, Fornasari et al. 2015).

Briefly, for random fibers, a 15% w/v GL solution was obtained in demineralized water at 50 °C and GPTMS were used as a GL crosslinker adding 137 µL GPTMS for each 1,5 g of GL and mixing for 1 hour before spinning. For aligned fibers, a small amount of PEO (90/10 volume ratio) was added to stabilize the polymer jet and to enhance aligned fibers formation.

CS 5 % (w/v) and 3% (w/v) PEO solutions were prepared separately by dissolving CS or PEO in 0.5 M acetic acid solution at room temperature by continuous stirring. After complete solubilization of each component, a 50/50 (v/v) CS/PEO solution was prepared by mixing equal volumes of CS and PEO solutions to obtain the mixtures with weight ratios of CS to PEO of 62/38; the resultant mixtures were kept under stirring about 2 hours. A 5% (v/v) of DMSO was added to the CS/PEO solution as a co-solvent to relax CS chain entanglements and to increase the fiber yields and consequently improving the spinnability of the CS-based solution (Bhattarai, Edmondson et al. 2005). To increase water stability of nano-fibers, a 1 M solution of DSP was added (CS/PEO_DSP) with a concentration of 7.5 % v/v with respect to the natural polymer solution volume as previously described by the authors (Ruini, Tonda-Turo et al. 2015). Uncrosslinked solution was prepared as control. The final solution was coded as CS. CS nano-fibers were prepared through electrospinning system using a voltage of 30kV, a temperature of 37 °C, a nozzle-collector distance of 12 cm and a flow rate of 30 µL/min. Randomly oriented nano-fibers were collected on a plane aluminum foil while for aligned nano-fibers a rotating mandrel with a speed of 2400 rpm was used.

Both GL and CS nano-fibers were collected on glass coverslips and then sterilized by overnight (O/N) exposure to UV irradiation (UV lamp Technoscientific Co., wavelength 254 nm) and then incubated O/N with complete DMEM (composition specified in 2.3 section), before proceeding with cell seeding.

2.2 Scanning electron microscopy and fibers morphology evaluation

Fibers morphology was investigated using Scansion Electronic Microscopy (SEM, LEO 1450VP). Prior to analysis samples were sputtered using gold under vacuum for 100 seconds by Agar Auto Sputter Coater. Then micrographs were analyzed through ImageJ software to measure fibers diameter.

The fiber mats wettability was measured using a KSV instrument equipped with CAM 200 software for data acquisition at room temperature. A 5 µl double distilled water droplet and the sessile drop method was applied. For each sample, at least five measurements on different surface area were acquired and results were expressed as an average value ± standard deviation.

The chemical composition of the fibers was detected through *Fourier transform infrared-attenuated total reflectance spectroscopy* (FTIR-ATR). The FTIR-ATR spectra

were recorded using a Perkin Elmer Spectrometer in the range of 2000‑600 cm^{-1} at a resolution of 4 cm^{-1}. Complete characterization of GL and CS nanofibers has been described in previous work (Tonda-Turo, Cipriani et al. 2013).

2.3 Cell cultures

RT4-D6P2T SC line and primary SCs were grown on monolayers at 37 °C in a humidified atmosphere of 5% CO_2 as previously described (Tonda-Turo, Cipriani et al. 2013; Gnavi, Fornasari et al. 2015). RT4-D6P2T cell line was purchased from ATCC (American Type Culture Collection, 10801 University Blvd, Manassas, VA 20110-2209) and grown, according to the ATCC protocol, in complete medium consisting of high glucose Dulbecco's modified Eagle's

medium (DMEM, Invitrogen) supplemented with 100 units ml^{-1} penicillin, 0.1 mg ml^{-1} streptomycin, 1 mM sodium pyruvate, 2 mM L-glutamine, 10% heat-inactivated foetal bovine serum (FBS, Invitrogen). SCs for primary culture were isolated from 3 cm of both sciatic nerves harvested from three adult female Wistar rat (Charles River Laboratories, Milan, Italy) weighing approximately 190-220 g. All procedures were in accordance with the European Communities Council Directive European Communities Council (2010/63/EU), with the National Institutes of Health guidelines, and with the Italian Law for Care and Use of Experimental Animals (DL26/14). Conformed measures were taken to minimize pain and discomfort taking human endpoints for animal suffering and distress into account. The sciatic nerves were harvested, purified and cultured as previously described (Gnavi, Fornasari et al. 2015; Gnavi, Fornasari et al. 2015). Briefly, the sciatic nerves were isolated, cut into 3 mm section and incubated at 37°C in 5% CO_2 in complete medium consisting of low glucose DMEM (Gibco) supplemented with 100 units ml^{-1} penicillin, 0.1 mg ml^{-1} streptomycin, 1 mM sodium pyruvate, 2 mM L-glutamine, 10% heat-inactivated foetal bovine serum (FBS, Invitrogen) 63 ng/ml glial growth factor (GGF, R&D Systems) and 10 µM forskolin (Sigma). The medium was changed every three days. After two weeks, 2 ml of digestion solution consisting of 0.6 mg/ml collagenase type IV (Sigma) and 0.5 mg/ml dispase (Invitrogen) diluted in low glucose complete medium were added. After 24 hours the incubated nerve segments were transferred to a 50 ml tube and suspended in 5 ml low glucose complete medium using a glass Pasteur pipette. The cell suspension was filtered through a 70 µm strainer (Falcon), centrifuged at 900 rpm for 5 minutes, re-suspended in 10 ml of complete DMEM medium and seeded on a poly-L-lysine (PLL, Sigma) coated plate. In order to remove contaminating fibroblasts, the confluent SCs were immunodepleted.

Briefly, the confluent SCs were harvested by trypsinization, re-suspended in 0.5 ml of low glucose complete medium containing mouse anti-rat Thy1.1 antibody diluted 1:500 (Serotec, MCA04G) and incubated for 10 min at 37°C. Fresh rabbit complement (0.25 ml, Cederlane Labs) was added and incubated for 30 minutes at 37°C. The reaction was blocked by adding 10 ml low glucose complete medium and 5 minutes centrifugation at 900 rpm. The pellet was re-suspended in low glucose complete medium and seeded on PLL-coated plates. Confluent cells were harvested twice a week by trypsinization and seeded at the desired dilution on a new plate.

2.4 Adhesion and proliferation assay: 4,6-diamidino-2-phenylindole immunocytochemical detection of proliferating cells.

RT4-D6P2T and primary SCs for adhesion assays were seeded in complete DMEM at 4000 and 8000 cells/cm^2 respectively. RT4-D6P2T and primary SCs for proliferation assays (4,6-diamidino-2-phenylindole immunocytochemical detection of proliferating cells) were seeded in complete DMEM at 1000 and 2000 cells/cm^2 respectively. Adhesion and proliferation assays were performed on both PLL- (control condition), random or aligned gelatin-fiber coated coverslips and random or aligned chitosan-fiber coated coverslips. After 3 hours (adhesion assay) 1, 3, 5, and 7 days (proliferation assay), cells were fixed, stained, photographed and counted. Briefly, culture medium was removed and the substrates with attached cells were rinsed with PBS before being fixed in 4% paraformaldehyde (PFA, Sigma-Aldrich) as described before (Tonda-Turo, Cipriani et al. 2013; Carriel, Scionti et al. 2015; Gnavi, Fornasari et al. 2015; Gnavi, Fornasari et al. 2015). After 20 minutes, the PFA solution was removed and the samples rinsed with PBS. The cells were permeabilized for 10 minutes with 0.1% Triton X-100 diluted in PBS and blocking solution (normal goat serum, NGS,

diluted 1:100 in PBS DAKO X0907) was added for 1 hour at room temperature. The cells were stained by O/N incubation with anti-vinculin rabbit polyclonal antibody (diluted 1:600 in PBS, Sigma), followed by 1 hour incubation with FITC-conjugated phalloidin at room temperature (diluted 1:1000 in PBS, Millipore) and goat-anti rabbit IgG (H + L) AlexaFluor488 (diluted 1:200 in PBS, Invitrogen). Nuclei were stained with 4,6-diamidino-2-phenylindole (DAPI, Sigma) diluted 1:1000 in PBS. Cells were photographed under an inverted fluorescence microscope Nikon Eclipse 80i equipped with a Nikon ECLIPSE 80i camera using Image-Pro Plus 6.0 (Media Cybernetics, Silver Spring, MD, USA). Cell numbers were calculated using ImageJ software, averaged and expressed as cells/mm^2 ± standard error of the mean (SEM). The experiments were repeated 3 times independently and included 5 sets of samples for each time-point. Each set included three control PLL-, three random gelatin fiber matrix-, three align gelatin fiber matrix-, three random chitosan fiber matrix-, and three align chitosan fiber matrix-coated coverslips.

2.5 MTT assay

RT4-D6P2T and primary SCs were plated in 0.2 ml of DMEM containing 10% FBS on both PLL- (control) and chitosan or gelatin random or aligned fibers (experimental group) as previously described (Tonda-Turo, Cipriani et al. 2013; Gnavi, Fornasari et al. 2015). In order to quantify the cell number serial dilutions were performed by plating 1×10^3, 2×10^3, 4×10^3, 8×10^3, 1.6×10^4, 3.2×10^4, and 6.4×10^4 per well. After a 1, 3, 5 and 7 day incubation, 10 µL MTT substrate (Sigma, 5 mg/ml in phosphate buffered saline) was added, and the cells incubated at 37 °C for 4 hours. The MTT solution was removed and cells washed twice with 0.1 ml of PBS. To dissolve formazan 0.1 ml of DMSO (Sigma) was added to each well.

Spectrophotometric absorbance was measured at 570 nm wavelength, using DMSO as the blank.

2.6 Evaluation of actin cytoskeleton organization

Cell adhesion and morphology were measured using immunocytochemistry staining against anti-vinculin and phalloidin. RT4-D6P2T and primary SCs were seeded, fixed and stained as described in paragraph 2.4. 3, 6 or 24 hour time points conditions have been performed has described before (Gnavi, Fornasari et al. 2015). For each sample 100 cells were examined making a total of 300 cells for each experimental condition. An arbitrary score was given to each cell and data were expressed as the percentage of cells displaying low, medium or high actin cytoskeleton organization or presence of focal adhesion points ± SEM. The entire procedure was carried out in a blind manner as previously described (Gnavi, Fornasari et al. 2015).

2.7 Estimation of lamellipodia and filopodia formation

Lamellipodia and filopodia formation was evaluated by direct microscopy of cells stained with anti-S-100β rabbit polyclonal antibody. The cells were seeded, fixed and stained as described in paragraph 2.4. 3, 6 or 24 hour time points conditions have been performed has described before (Gnavi, Fornasari et al. 2015). For each sample, 100 cells were examined, making a total of 300 cells for each experimental condition. The data were expressed as percentages of cells displaying only lamellipodia or lamellipodia and filopodia ± SEM. The entire procedure was carried out in a blind manner as previously described (Gnavi, Fornasari et al. 2015).

2.8 50B11 cultures and differentiation

To visualize individual neurite growth, cells were plated at low densities on both PLL-(control), random or aligned gelatin-fiber coated coverslips and random or aligned chitosan-fiber coated coverslips. Twenty-four hours after plating, cells were differentiated by adding forskolin (Sigma-Aldrich, 75 μM) to the culture medium as previously described (Gnavi, Fornasari et al. 2015). Twenty-four hours after differentiation, cells were fixed, stained and as described in paragraph 2.4, using β-tubulin mouse mAb (diluted 1:100, in PBS, Sigma) and goat-anti-mouse IgG (H + L) Cy3 (diluted 1:200 in PBS, Invitrogen). Nuclei were stained with DAPI (diluted 1:1000 in PBS, Sigma). Cell number and axon lengths were measured using ImageJ software. Cell number and percentages of differentiated or undifferentiated cells were evaluated in both differentiated and undifferentiated conditions. Counted cells for each assay were averaged and expressed as cells/mm^2 ± SEM. Axon length was expressed in μm ± SEM.

2.9 DRG explants

DRG explants were harvested from adult female Wistar rats (Charles River Laboratories, Milan, Italy) weighing approximately 190–220 g. All procedures were in accordance with the European Communities Council Directive European Communities Council (2010/63/EU), with the National Institutes of Health guidelines, and with the Italian Law for Care and Use of Experimental Animals (DL26/14). Conformed measures were taken to minimize pain and discomfort taking human endpoints for animal suffering and distress into account. Explants were cultured on coverslips coated with the different fibers matrices. Matrigel coated coverslips were used as negative control. In order to avoid the detachment of the explants

100 µl matrigel® were added to the top of the cultures. After 1 hour of incubation at 37 °C to allow the matrigel® to polymerize, complete F12-BME medium (2 ml) was added. Complete F12–BMEmedium is composed by F12 and BME media (Gibco) in a 50:50 ratio containing 1% bovine serum albumin (BSA, Sigma), 0.5 g/ml D-glucose (Sigma), 100 U/ml penicillin and streptomycin (Sigma), 1 mg/100 ml putrescine (Sigma), 2 mM L-glutamine (Sigma), 2 ml of 100× insulin–selenium–transferrin (Gibco) and 0.125 ng/ml vitamin C. Culture medium was added, either without growth factors (negative control) or containing 50 ng NGF/ml (positive control, Millipore).

After 48 hour of incubation, the explants were fixed with 4% PFA, for 20 min at room temperature. Axons were stained immunocytochemically as described in paragraph 2.4, using β-tubulin mouse mAb (diluted 1:100, in PBS, Sigma) and goat-anti-mouse IgG (H + L) AlexaFluor488 (diluted 1:200 in PBS, Invitrogen). Nuclei were stained with DAPI (diluted 1:1000 in PBS, Sigma). For quantification, whole explants were acquired through an inverted optical video-confocal microscope (ViCo, Nikon Eclipse 80i) equipped with a Nikon ECLIPSE 80i camera using Image-Pro Plus 6.0 (Media Cybernetics USA). Axon density, sprouting area and axon lengths were measured using by ImageJ software as described elsewhere (Zamburlin, Gilardino et al. 2006; Gilardino, Farcito et al. 2009). Axon density was expressed as pixels occupied by axons ± SEM. Sprouting area was expressed as the ratio between DRG axon occupied area and DRG body area ± SEM. Axon length was expressed in µm ± SEM.

2.10 Confocal microscopy

Samples were observed with a Nikon Eclipse E800 epifluorescence microscope under appropriate filters and a Leica TCS SP5 confocal laser scanning microscope (Leica,

Mannheim, Germany) using a 40× Plan-NEOFLUAR objective (numerical aperture (NA) = 1.25) or 63× Plan-NEOFLUAR objective (numerical aperture (NA) = 1.40). High-resolution images were acquired (1024 × 1024 pixels) at 100 Hz.

2.11 Statistics

The experiments were repeated 3 times independently (biological triplicate) and included 5 sets of samples. Each set (technical triplicate) included three control PLL-, three random gelatin fiber matrix-, three align gelatin fiber matrix-, three random chitosan fiber matrix-, and three align chitosan fiber matrix-coated coverslips for each time point or growth factor condition. The data are expressed as mean ± SEM. GraphPad Prism® software was used for one or two-way analysis of variance (ANOVA). Values of * $p < 0.05$, ** $p < 0.01$, *** $p < 0.001$ were considered statistically significant.

3. RESULTS AND DISCUSSION

3.1 Gelatin and chitosan polymer can be easily used to prepare electrospun nano-fibers

GL and CS nano-fibers were obtained with no defects on the fiber surface **(Figure 1).** Despite the differences in materials and parameters used, the average diameter of the different fibers was similar and did not show significant differences **(Table 1).** A slight reduction of CS wettability compared to GL was detected due to the lower hydrophilicity of CS compared to GL. The FTIR-ATR spectra **(Figure 2)** show the characteristic peaks of the constituent materials as reported in **tables 2 and 3.** No differences were observed for randomly oriented and aligned fibers and data were reported only for randomly oriented samples.

3.2 Gelatin and chitosan nano-fibers promote similar Schwann cells adhesion rate

RT4-D6P2T cells and primary SCs were cultured on poly-l-lysine coated coverslips (control condition), gelatin and chitosan random and aligned fibers. After 3 hours, the adherent cells were fixed, stained and counted. The alignment of gelatin and chitosan electrospun fibers decreased the number of adherent cells for RT4-D6P2T and primary SC cultures **(Figure 3).** RT4-D6P2T cells seeded on aligned gelatin fibers displayed lower adhesion rate than under control conditions ($p<0.05$), gelatin random fibers ($p<0.01$), and chitosan random fibers ($p<0.05$) **(Figure 3).** RT4-D6P2T cells seeded on aligned chitosan fibers displayed lower adhesion rate than under control conditions ($p<0.01$), gelatin random fibers ($p<0.01$), and chitosan random fibers ($p<0.05$) **(Figure 3).**

Primary SCs seeded on aligned gelatin fibers displayed lower adhesion rate than under control conditions ($p<0.001$), gelatin random fibers ($p<0.001$), and chitosan random fibers ($p<0.01$) **(Figure 3).** Primary SCs seeded on aligned chitosan fibers displayed lower adhesion rate than under control conditions ($p<0.001$), gelatin random fibers ($p<0.001$), and chitosan random fibers ($p<0.001$) **(Figure 3).** Moreover, primary SCs seeded on chitosan aligned fibers displayed lower adhesion rate in comparison to gelatin aligned fibers ($p<0.05$) **(Figure 3).** All together these results showed that gelatin and chitosan random fibers promote SC adhesion reaching adhesion rate levels similar to cells cultured on control condition. Aligned fibers still promote SC adhesion even if adhesion rates are lower than those reached by cells cultured on control condition and random fibers. This can be due to the different topography of the aligned fibers in comparison to the random ones (Bacakova, Filova et al. 2011; Rahmany and Van Dyke 2013).

Particularly, fibers alignment provides less contact points to the cells thus resulting in lower adhesion rate (Bacakova, Filova et al. 2011; Rahmany and Van Dyke 2013; Gnavi, Fornasari et al. 2015). On the other hand, random fibers distribution results in a complex network formation between fibers providing many contact points to the adhering cells (Bacakova, Filova et al. 2011; Harvey, Hill et al. 2013; Rahmany and Van Dyke 2013; Gnavi, Fornasari et al. 2015). Concerning cell morphology, fiber alignment results in adherent cells aligning their body to the direction of the fiber whereas cells seeded on random fibers display a spread morphology in accordance with previous study (Cirillo, Guarino et al. 2014; Gnavi, Fornasari et al. 2015; Gnavi, Fornasari et al. 2015).

3.3 Chitosan nano-fibers resulted in lower Schwann cell proliferation rate in comparison with gelatin nano-fibers

RT4-D6P2T cells and primary SCs were cultured on poly-l-lysine coated coverslips (control condition), gelatin and chitosan random fibers and aligned fibers. After 1, 3, 5 and 7 *days in vitro* (DIV) the proliferating cells were fixed, stained and counted **(Figures 4 and 5).** The alignment of gelatin and chitosan electrospun fibers decreased the number of proliferating cells for RT4-D6P2T and primary SC cultures (**Figures 4 and 5** respectively). Moreover, RT4-D6P2T and primary SCs displayed lower proliferation rate when cultured on chitosan fibers, both random and aligned in comparison to control condition and random gelatin fibers. Two-way Anova analysis reported in **supplementary table 1** show that the different fiber substrate ($p<0.001$) and the time ($p<0.001$) affect RT4-D6P2T cell proliferation. Interaction between the different fiber

substrates and time accounts 13.04% of the total variance affecting significantly cell proliferation ($p<0.001$).

Particularly, RT4-D6P2T cells seeded on random gelatin fibers, aligned gelatin fibers, or aligned chitosan fibers displayed lower proliferation rate than under control condition and gelatin random fibers both at 5 and 7 DIV ($p<0.001$), and chitosan random fibers ($p<0.05$) (Two-way Anova analysis is reported in **supplementary table 1)**. RT4-D6P2T cells seeded on aligned chitosan fibers displayed lower proliferation rate than under gelatin aligned fibers at 5 ($p<0.05$) and 7 ($p<0.001$) DIV (Two-way Anova analysis is reported in **supplementary table 1)**. Finally, RT4-D6P2T cells seeded on aligned chitosan fibers displayed lower proliferation rate than under chitosan random fibers at 5 ($p<0.01$) and 7 ($p<0.001$) DIV (Two-way Anova analysis is reported in **supplementary table 1)**. Similar results have been obtained by using primary SC cultures **(Figure 5),** Two-way Anova analysis is reported in the **Supplementary table 2).**

In order to evaluate cell vitality, MTT assay has been performed on both RT4-D6P2T cells and primary SCs cultured on the different substrates **(Figures 4v and 5v).** MTT results are in agreement with proliferation assay data for both RT4-D6P2T cells and primary SCs (MTT assay Two-way ANOVA results for RT4-D6P2T and primary SCs are reported in **supplementary table 3 and 4, respectively)**. All together proliferation and MTT assay results demonstrate that the different substrates allow SC proliferation and vitality in agreement with previous data (Gnavi, Fornasari et al. 2015; Gnavi, Fornasari et al. 2015). Although, random gelatin fibers seems to be the better substrate for SC proliferation and vitality followed by gelatin aligned fibers, chitosan random fibers and chitosan aligned fibers. The higher cell proliferation on random fibers can be due to the fibers

topography that, as already discussed, provides more contact points to the proliferating cells (Bacakova, Filova et al. 2011; Harvey, Hill et al. 2013; Rahmany and Van Dyke 2013). Even if random fibers induce higher proliferation rate, a number of study reported that fibers alignment promotes better nerve regeneration (Neal, Tholpady et al. 2012; Gnavi, Barwig et al. 2013; Cirillo, Guarino et al. 2014; Huang, Ouyang et al. 2015). Particularly, fluorescent images show that SCs cultured on aligned fibers arrange themselves in parallel bands with elongate cell body parallel to the direction of the fibers. Thus, aligned fibers can be use to promote band of Bungner formation *in vivo* enhancing nerve regeneration processes (de Ruiter, Malessy et al. 2009; Deumens, Bozkurt et al. 2010).

3.4 Gelatin and chitosan nano-fibers alignment resulted in lower actin cytoskeleton organization and fewer focal adhesion points in comparison with gelatin nano-fibers

Both RT4-D6P2T cells **(Figure 6)** and primary SCs **(Figure 7)** cultured under control conditions and on aligned and random gelatin and chitosan fibers. Cells seeded on control conditions and random gelatin fibers displayed higher actin cytoskeleton organization and many focal adhesion points than those cultured on gelatin aligned fibers and chitosan fibers both random and aligned. This trend was maintained at all the time points tested (3, 6 and 24 hours). Two-way Anova analysis is reported in **supplementary table 11-16** for RT4-D6P2T cells and in **supplementary table 17-22** for primary SCs. Finally, actin cytoskeleton staining showed that cells cultured under control conditions (Figure5-6 a, f, k, p) and on gelatin random fibers (Figure5-6 b, g, l, q) displayed a spread morphology whereas those cultured on aligned and chitosan fibers had an elongated morphology. These data agreed with the adhesion assay results and

with previous studies (Cirillo, Guarino et al. 2014; Gnavi, Fornasari et al. 2015; Gnavi, Fornasari et al. 2015). Several authors reported that actin cytoskeleton organization plays an important role in lamellipodia and filipodia formation (Parsons, Horwitz et al. 2010; Mullins and Hansen 2013). Since a different actin cytoskeleton organization on SCs cultured on the different substrates has been observed immunofluorescence assays to investigate if there were differences on lamellipodia and filipodia formation on the different substrates have been performed.

3.5 Gelatin and chitosan nano-fibers alignment enhances filopodia formation

Lamellipodia and filipodia formation has been evaluated by culturing both RT4-D6P2T cell line and primary SC on the different substrates. Results showed that fiber alignment led to more cells displaying filopodia in both RT4-D6P2T cells **(Figure 8)** and primary SCs **(Figure 9).** This trend was maintained at all the time points tested (3, 6 and 24 h, Figure 7-8 f, g and h respectively). Two-way Anova analysis is reported in **Supplementary table 23-25 and 26-28** for RT4-D6P2T cells and primary SCs respectively). Lamellipodia are motile structures formed by a thin sheet of cytoplasm filled with a criss-cross arranged network of actin filaments. Filopodia consist of rod-shaped cell projections full of linear actin filaments and their formation often is associated with lamellipodia formation. Several studied reported that filipodia formation is associated to cell motility and migration (Qu 2013), thus our data suggest that fiber alignment may induce SC migration.

3.6 Gelatin nano-fibers resulted in higher 50B11 cell differentiation and neurites length in comparison with chitosan nano-fibers

50B11 cells were seeded under control condition, and on aligned and random gelatin and chitosan fibers. After 24 hours, 50B11 cells displayed high adhesion rate under the different substrates without any statistical difference between groups **(Supplementary table 8).** The alignment of gelatin and chitosan fibers did not affect the number of adherent 50B11 cells **(Figure 10p).** Addition of forskolin resulted in 50B11 differentiation under all tested conditions **(Figure 10p)** without any statistical differences **(Supplementary table 8).** After forskolin addition, 50B11 cells stopped to proliferate and started to differentiate, resulting in a reduction of cell number compared with non-treated conditions (One-way Anova statistical analysis is reported in **Figure 10**). The number of differentiated 50B11 cells is slightly decreased when 50B11 cells are cultured on gelatin aligned fibers in comparison to control conditions ($p<0.05$). 50B11 neurite length was higher on control conditions, gelatin random fibers and gelatin aligned fibers in comparison to chitosan random and aligned fibers **(Figure 10 q).** According with these results, confocal images showed that aligned fibers made neurites parallel to the direction of the fibers **(Figure 10 c, h, and m; Figure 10 e, j, and o for gelatin and chitosan fibers respectively**). In order to understand if fibers themselves can induce cell differentiation the number of differentiated cells was evaluated in presence or absence of forskolin in culture medium**.** Results, expressed as percentage of differentiated and undifferentiated cells, show that with forskolin addition **(Figure 10 r)** there are high percentages of differentiated cells without any statistical differences between the different substrates **(Supplementary table 9).** When 50B11 cells are cultured without

forskolin there are higher percentages of undifferentiated cells **(Figure 10 s).** Although gelatin aligned fibers seems to induce 50B11 differentiation in comparison with control conditions, gelatin random fibers and, chitosan random and aligned fibers ($p<0.001$) **(Supplementary Table 10).** These results suggest that gelatin random and aligned fibers topography may induce neuron differentiation and neurite alignment in agreement with several studies (Xie, MacEwan et al. 2009; Mahairaki, Lim et al. 2011; Cirillo, Guarino et al. 2014; Gnavi, Fornasari et al. 2015; Huang, Ouyang et al. 2015). Particularly, longitudinally aligned nano-fibers promote ordered neurites outgrowth (Huang, Ouyang et al. 2015), PC12 and DRGs alignment and parallel axonal growth and hMSC and PC-12 cells neurogenic differentiation (Cirillo, Guarino et al. 2014).

3.7 Gelatin and chitosan nano-fibers resulted in similar DRG neurites growth and alignment

DRG explants were cultured on poly-l-lysine coated coverslips (control condition), gelatin and chitosan random fibers and aligned fibers with or without NGF in culture medium. After 48 hours, the explants were fixed, stained and neurite length, neurite occupied area and neurite area ratio were quantified. Neurite length, neurite occupied area and neurite area ratio were higher when DRG explants were cultured in presence of NGF (One-way Anova statistical analysis is reported in F**igure 11).** When DRG explants were cultured in presence of NGF neurite length was higher on gelatin and chitosan aligned fibers in comparison with all the other tested conditions **(Figure 11 f and Supplementary table 5).** There are no differences between neurite length of DRG explants cultured on gelatin and chitosan aligned fibers in presence of NGF **(Supplementary table 5).**

Moreover, when DRG explants were cultured without NGF, neurite length was higher on gelatin aligned fibers, chitosan random and aligned fibers in comparison to control conditions and gelatin random fibers **(Supplementary table 5).**

When DRG explants were cultured in presence of NGF neurite occupied area was higher on control condition and random fibers in comparison to aligned fibers **(Figure 11 g and Supplementary table 6)**. When DRG explants were cultured without NGF neurite occupied area was lower on control condition and aligned fibers in comparison with the other tested substrate **(Supplementary table 6)**. Similar results have been obtained by evaluating the ratio between the area occupied by the neurites and the area occupied by the DRG bodies **(Figure 11 h and Supplementary table 7).** Fluorescence images **(Figure 11 c and e)** show that aligned fibers result in parallel neurites outgrowth in agreement with literature data (Xie, MacEwan et al. 2009; Cirillo, Guarino et al. 2014).

CONCLUSION

Reported data show that both gelatin and chitosan fibers can be promising filler for peripheral nerve conduits development. Particularly, aligned fibers induce SCs and axon oriented growth with cell body parallel to the direction of the fibers. DRG neurite outgrowth was similar on the different tested substrates. Although, gelatin fibers resulted in higher 50B11 neuronal differentiation in comparison to chitosan fibers. Concerning chitosan fibers we observed an oriented SCs and neurite growth that can be due to both the polymer biomimetic and biochemical intrinsic properties of the material (Gnavi, Barwig et al. 2013; Meyer, Stenberg et al. 2016). Both chitosan and gelatin have been widely used for peripheral nerve repair displaying high biocompatibility (Ciardelli and Chiono 2006; Chiono, Tonda-Turo et al. 2009; Foster and Karsten 2012; Gnavi, Barwig et al. 2013; Huang, Ouyang

et al. 2015; Meyer, Stenberg et al. 2016). In this work gelatin and chitosan fibers have been tested showing that depending on their morphology and biochemical composition they can induce and promote different regenerative events (i.e. SC adhesion, SC proliferation, neuronal differentiation and growth). In conclusion, although *in vitro* positive results not always are predictors of a similar *in vivo* performances (Gomes, Rodrigues et al. 2015), our data support that all the tested substrates are potential candidates for nerve reconstruction

.

ACKNOWLEDGMENTS

We thank Ahmet Höke (Department of Neurology, School of Medicine, Johns Hopkins University, Baltimore, USA) for providing the 50B11 cell line. We acknowledge a research grant for Sara Gnavi from the Franco and Marilisa Caligara Foundation. This work also received funding from the European Community's Seventh Framework Programme (FP7-HEALTH-2011) under grant agreement n 278612 (BIOHYBRID).

REFERENCES

Adomaviciute, E. and R. Milasius (2007). "The influence of applied voltage on poly(vinyl alcohol) (PVA) nanofibre diameter." Fibres & Textiles in Eastern Europe **15**(5-6): 69-72.

Agarwal, S. W., H. Greiner, A. (2008). "Use of electrospinning technique for biomedical applications." Polymer **49**: 5603-5621.

Bacakova, L., E. Filova, et al. (2011). "Modulation of cell adhesion, proliferation and differentiation on materials designed for body implants." Biotechnol Adv **29**(6): 739-767.

Bhardwaj, N. and S. C. Kundu (2010). "Electrospinning: a fascinating fiber fabrication technique." Biotechnol Adv **28**(3): 325-347.

Bhattarai, N., D. Edmondson, et al. (2005). "Electrospun chitosan-based nanofibers and their cellular compatibility." Biomaterials **26**(31): 6176-6184.

Biazar, E., M. T. Khorasani, et al. (2010). "Types of neural guides and using nanotechnology for peripheral nerve reconstruction." Int J Nanomedicine **5**: 839-852.

Carriel, V., M. Alaminos, et al. (2014). "Tissue engineering of the peripheral nervous system." Expert Rev Neurother **14**(3): 301-318.

Carriel, V., G. Scionti, et al. (2015). "In vitro characterization of a nanostructured fibrin agarose bio-artificial nerve substitute." J Tissue Eng Regen Med.

Chiono, V., C. Tonda-Turo, et al. (2009). "Chapter 9: Artificial scaffolds for peripheral nerve reconstruction." Int Rev Neurobiol **87**: 173-198.
Christopherson, G. T., H. Song, et al. (2009). "The influence of fiber diameter of electrospun substrates on neural stem cell differentiation and proliferation." Biomaterials **30**(4): 556-564.
Ciardelli, G. and V. Chiono (2006). "Materials for peripheral nerve regeneration." Macromol Biosci **6**(1): 13-26.
Cirillo, V., V. Guarino, et al. (2014). "Optimization of fully aligned bioactive electrospun fibers for "in vitro" nerve guidance." J Mater Sci Mater Med **25**(10): 2323-2332.
Dahlin, L. B., L. Anagnostaki, et al. (2001). "Tissue response to silicone tubes used to repair human median and ulnar nerves." Scand J Plast Reconstr Surg Hand Surg **35**(1): 29-34.
Daly, W., L. Yao, et al. (2012). "A biomaterials approach to peripheral nerve regeneration: bridging the peripheral nerve gap and enhancing functional recovery." J R Soc Interface **9**(67): 202-221.
de Ruiter, G. C., M. J. Malessy, et al. (2009). "Designing ideal conduits for peripheral nerve repair." Neurosurg Focus **26**(2): E5.
Deumens, R., A. Bozkurt, et al. (2010). "Repairing injured peripheral nerves: Bridging the gap." Prog Neurobiol **92**(3): 245-276.
Foster, L. J. R. and E. Karsten (2012). "A Chitosan Based, Laser Activated Thin Film Surgical Adhesive, 'SurgiLux': Preparation and Demonstration." Jove-Journal of Visualized Experiments(68).
Gilardino, A., S. Farcito, et al. (2009). "Specificity of the second messenger pathways involved in basic fibroblast growth factor-induced survival and neurite growth in chick ciliary ganglion neurons." J Neurosci Res **87**(13): 2951-2962.
Gnavi, S., C. Barwig, et al. (2013). "The use of chitosan-based scaffolds to enhance regeneration in the nervous system." Int Rev Neurobiol **109**: 1-62.
Gnavi, S., B. E. Fornasari, et al. (2015). "The influence of electrospun fibre size on Schwann cell behaviour and axonal outgrowth." Mater Sci Eng C Mater Biol Appl **48**: 620-631.
Gnavi, S., B. E. Fornasari, et al. (2015). "The Effect of Electrospun Gelatin Fibers Alignment on Schwann Cell and Axon Behavior and Organization in the Perspective of Artificial Nerve Design." Int J Mol Sci **16**(6): 12925-12942.
Gomes, S. R., G. Rodrigues, et al. (2015). "In vitro and in vivo evaluation of electrospun nanofibers of PCL, chitosan and gelatin: a comparative study." Mater Sci Eng C Mater Biol Appl **46**: 348-358.
Gu, X., F. Ding, et al. (2011). "Construction of tissue engineered nerve grafts and their application in peripheral nerve regeneration." Prog Neurobiol **93**(2): 204-230.
Harvey, A. G., E. W. Hill, et al. (2013). "Designing implant surface topography for improved biocompatibility." Expert Rev Med Devices **10**(2): 257-267.
Huang, C., Y. Ouyang, et al. (2015). "Nerve guidance conduits from aligned nanofibers: improvement of nerve regeneration through longitudinal nanogrooves on a fiber surface." ACS Appl Mater Interfaces **7**(13): 7189-7196.
Ichihara, S., Y. Inada, et al. (2008). "Artificial nerve tubes and their application for repair of peripheral nerve injury: an update of current concepts." Injury **39 Suppl 4**: 29-39.
Khor, E. and L. Y. Lim (2003). "Implantable applications of chitin and chitosan." Biomaterials **24**(13): 2339-2349.
Mahairaki, V., S. H. Lim, et al. (2011). "Nanofiber matrices promote the neuronal differentiation of human embryonic stem cell-derived neural precursors in vitro." Tissue Eng Part A **17**(5-6): 855-863.
Meyer, C., L. Stenberg, et al. (2016). "Chitosan-film enhanced chitosan nerve guides for long-distance regeneration of peripheral nerves." Biomaterials **76**: 33-51.

Mullins, R. D. and S. D. Hansen (2013). "In vitro studies of actin filament and network dynamics." Curr Opin Cell Biol **25**(1): 6-13.
Neal, R. A., S. S. Tholpady, et al. (2012). "Alignment and composition of laminin-polycaprolactone nanofiber blends enhance peripheral nerve regeneration." J Biomed Mater Res A **100**(2): 406-423.
Parsons, J. T., A. R. Horwitz, et al. (2010). "Cell adhesion: integrating cytoskeletal dynamics and cellular tension." Nat Rev Mol Cell Biol **11**(9): 633-643.
Qu, J. W., D. Wang, H. Dong, Y. Zhang, F. Zuo, B. Zhang, H. (2013). "Electrospun silk fibroin nanofibers in different diameters support neurite outgrowth and promote astrocyte migration." J Biomed Mater Res Part A **101A**: 2667–2678.
Rahmany, M. B. and M. Van Dyke (2013). "Biomimetic approaches to modulate cellular adhesion in biomaterials: A review." Acta Biomater **9**(3): 5431-5437.
Ruini, F., C. Tonda-Turo, et al. (2015). "Chitosan membranes for tissue engineering: comparison of different crosslinkers." Biomed Mater **10**(6): 065002.
Siemionow, M. and G. Brzezicki (2009). "Chapter 8: Current techniques and concepts in peripheral nerve repair." Int Rev Neurobiol **87**: 141-172.
Tonda-Turo, C., E. Cipriani, et al. (2013). "Crosslinked gelatin nanofibres: preparation, characterisation and in vitro studies using glial-like cells." Mater Sci Eng C Mater Biol Appl **33**(5): 2723-2735.
Xie, J., M. R. MacEwan, et al. (2009). "Neurite outgrowth on nanofiber scaffolds with different orders, structures, and surface properties." ACS Nano **3**(5): 1151-1159.
Yarin, A. L., S. Koombhongse, et al. (2001). "Bending instability in electrospinning of nanofibers." Journal of Applied Physics **89**(5): 3018-3026.
Zamburlin, P., A. Gilardino, et al. (2006). "Temporal dynamics of neurite outgrowth promoted by basic fibroblast growth factor in chick ciliary ganglia." J Neurosci Res **84**(3): 505-514.
Zhang, B. G., A. F. Quigley, et al. (2014). "Recent advances in nerve tissue engineering." Int J Artif Organs **37**(4): 277-291.
Zhang, S., Y. Huang, et al. (2009). "Gelatin nanofibrous membrane fabricated by electrospinning of aqueous gelatin solution for guided tissue regeneration." J Biomed Mater Res A **90**(3): 671-679.

	GL random fibers	GL aligned fibers	CS random fibers	CS aligned fibers
Fiber size (nm)	242± 35nm	204 ± 48 nm	167 ± 34 nm	159± 41 nm
Contact angle (°)	37±5	44±3	49±7	56±4

Table 1. Average size and contact angle of GL and CS nano-fibers.

GL nano-fibers		
Bond Vibration		*Wave Number (cm^{-1})*
GL	νO-H	3285,24
GL	Amide B	2937,99
GL - PEO	τC-H	2870,23
GL	νC=O	1635,79
GL	δN-H	1534,83
PEO	δCH_2	1470,20
PEO	ωCH_2	1360,31
PEO	τCH_2	1279,41 – 1241,56
GL - PEO	νC-N e δN-H	1241,76
GPTMS	Si-O-Si	1031,36 – 1160,51
PEO	ρCH_2	969,47 – 951,3
GPTMS	νSi-OH	916,12
GPTMS	Cyclic epoxide	871,21

Table 2. FTIR peaks related to GL nano-fibers.

CS nano-fibers		
Bond Vibration		*Wave Number (cm^{-1})*
CS	νO-H νN-H	3221,59
CS/PEO	νC-H	2882,98
CS	νC=O	1633,56
CS	δN-H	1546,59
PEO	δCH_2	1466,39
CS	νC-N	1409,64
PEO	ωCH_2	1359,79
PEO	τCH_2	1279,5 – 1241,07
CS - PEO	νC-O-C	1148,45 – 1095,02 – 1060,08
PEO	ρCH_2	959,44 – 947,03
PEO	δC-O-C	841,87
DSP	νPO_3	1059,30
DSP	δO-P-O	944,65

Table 3. FTIR peaks related to CS nano-fibers.

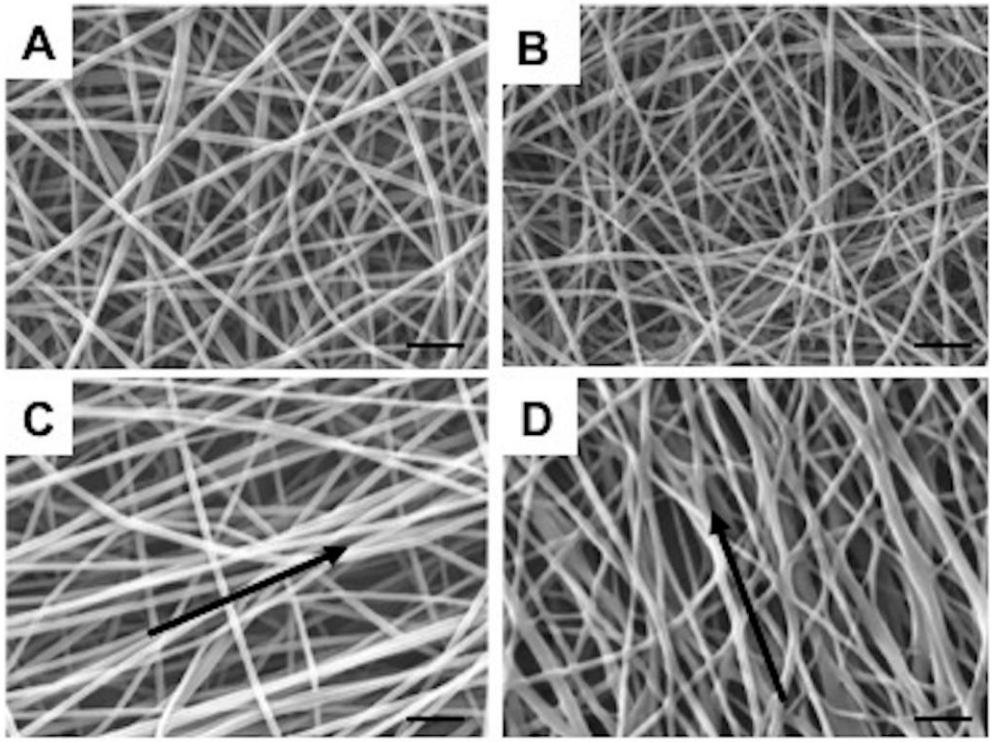

Figure 1. SEM micrographs of randomly oriented GL (A) and CS (B) nano-fibers and of aligned GL (C) and (D) CS nano-fibers. Scale bars: 2 μm.

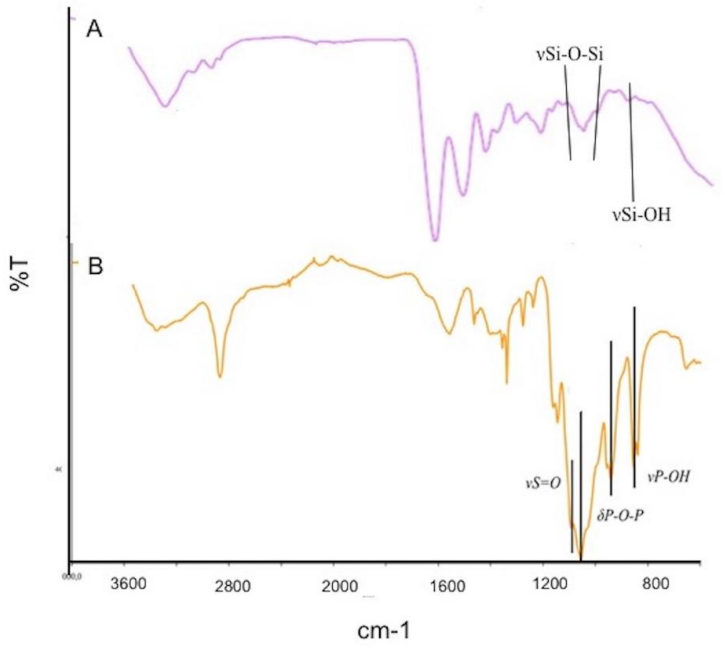

Figure 2. FTIR spectra.

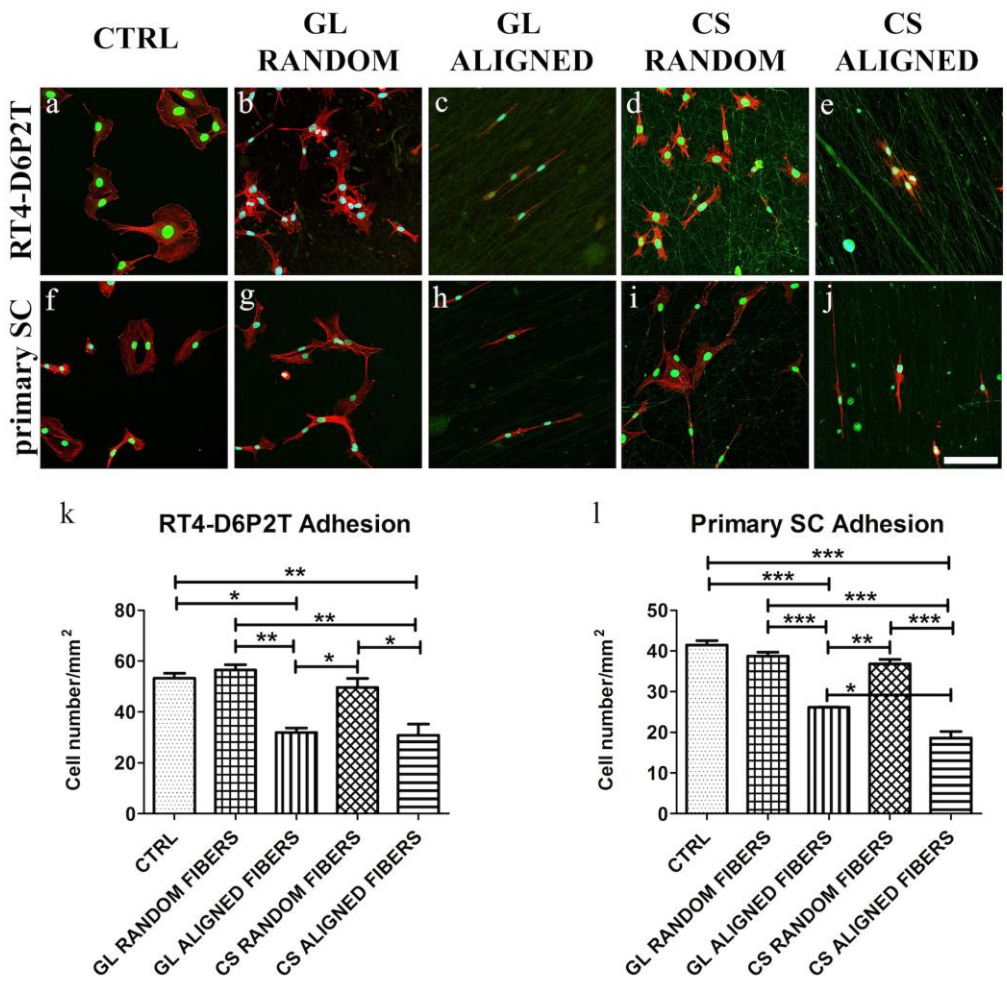

Figure 3. Adhesion assay. Fluorescence images after vinculin (green), phalloidin (red) and DAPI (blue) staining of RT4-D6P2T (a-e) and primary SC culture (f-j) on poly-l-lysine coated coverslips (control condition, a and f), gelatin random fibers (b and g), gelatin aligned fibers (c and h), chitosan random fibers (d and i), and chitosan aligned fibers (e and j). Fibers substrates appear green due to material autofluorescence. Images were acquired at 40X magnification. Scale bar: 100 μm. Number of adhering RT4- D6P2T (k) and primary SC cells (l) are reported. Cell number is expressed as cells/mm2 ☐} standard error of the mean (SEM). One-way ANOVA was used for statistical analysis. Asterisks denote statistically significant differences with *p ≤ 0.05, **p ≤ 0.01 and ***p ≤ 0.001.

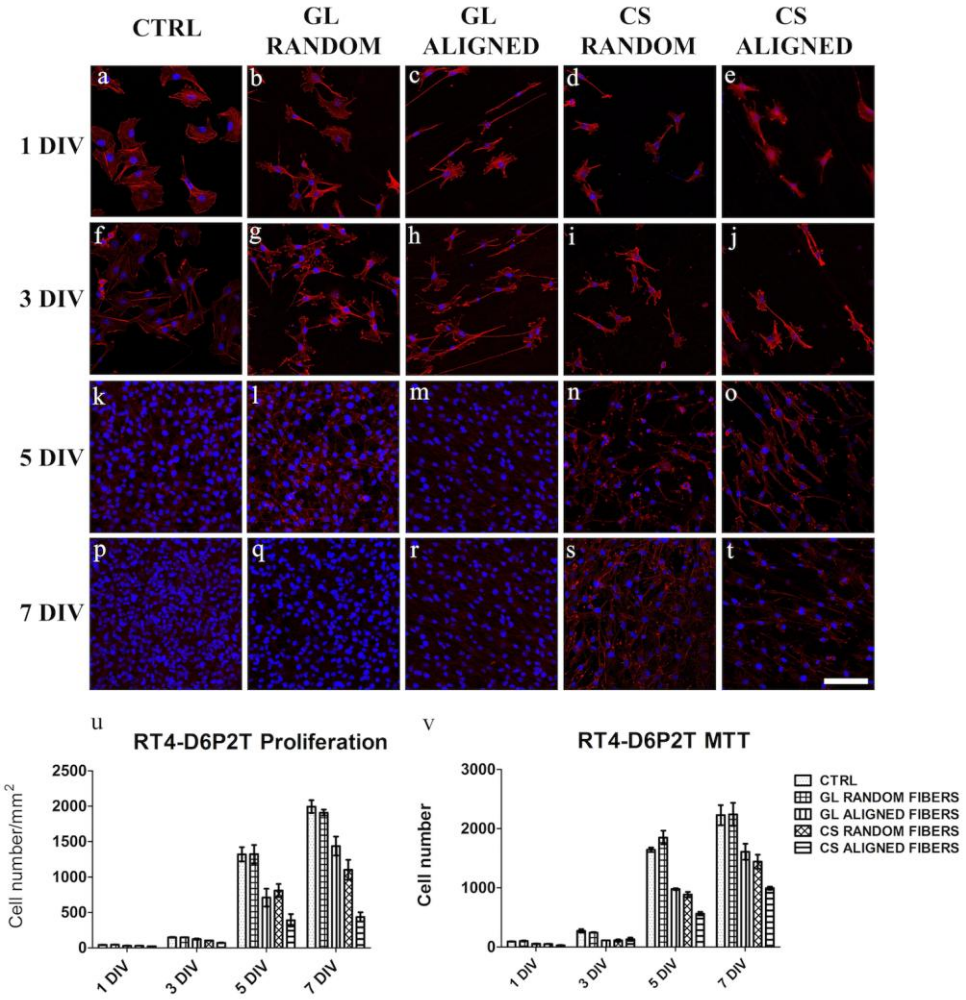

Figure 4. RT4-D6P2T proliferation and MTT assay. Fluorescence images after phalloidin (red) and DAPI (blue) staining of RT4-D6P2T (a-t), on poly-l-lysine coated coverslips (control condition, a, f, k, and p), gelatin random fibers (b, g, l, and q), gelatin aligned fibers (c, h, m, and r), chitosan random fibers (d, i, n, and s), and chitosan aligned fibers (e, j, o, and t) after 1 (a-e), 3 (f-j), 5 (k-o) and 7 (p-t) DIV (days in vitro). Images were acquired at 40X magnification. Scale bar: 100 μm. Number of proliferating RT4-D6P2T is reported as cells/mm2 ☐} standard error of the mean (SEM) (u). Cell vitality was quantified trough MTT assay and reported as cell number☐} SEM (v). Two-way ANOVA was used for statistical analysis *p ≤ 0.05, **p ≤ 0.01 and ***p ≤ 0.001 (Supplementary table 1 and 3).

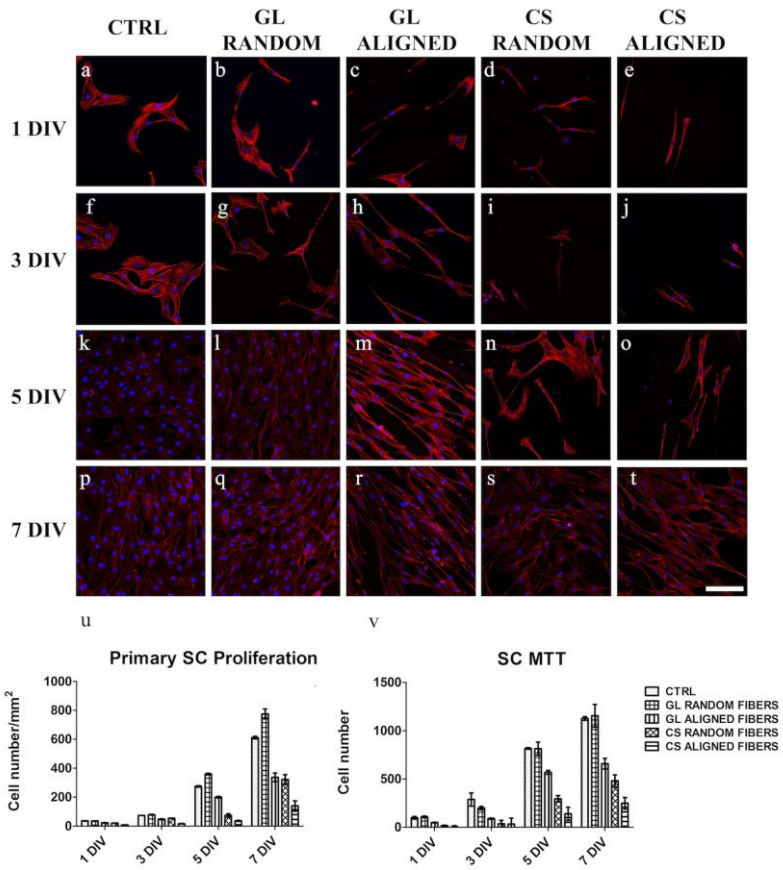

Figure 5. Primary SC proliferation and MTT assay. Fluorescence images after phalloidin (red) and DAPI (blue) staining of SC (a-t), on poly-l-lysine coated coverslips (control condition, a, f, k, and p), gelatin random fibers (b, g, l, and q), gelatin aligned fibers (c, h, m, and r), chitosan random fibers (d, i, n, and s), and chitosan aligned fibers (e, j, o, and t) after 1 (a-e), 3 (f-j), 5 (k-o) and 7 (p-t) DIV (days in vitro). Images were acquired at 40X magnification. Scale bar: 100 μm. Number of proliferating SC is reported as cells/mm2 □} standard error of the mean (SEM) (u). Cell vitality was quantified trough MTT assay and reported as cell number□} SEM (v). Two-way ANOVA was used for statistical analysis *p ≤ 0.05, **p ≤ 0.01 and ***p ≤ 0.001 (Supplementary tables 2 and 4).

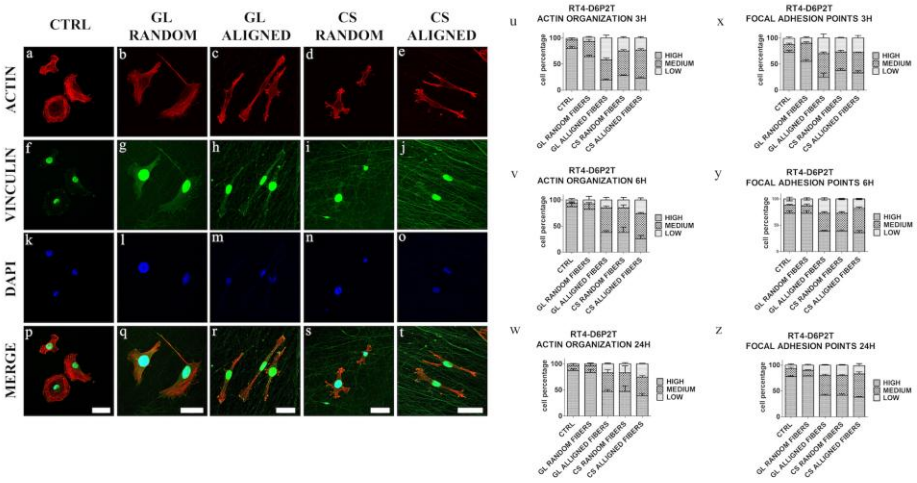

Figure 6. RT4-D6P2T actin cytoskeleton and focal adhesion points organization. Fluorescence images following phalloidin-actin (red), vinculin (green) and DAPI (blue) staining of RT4-D6P2T on poly-l-lysine coated coverslips (control condition, a, f, k and p), gelatin random fibers (b, g, l and q), gelatin aligned fibers (c, h, m and r), chitosan random fibers (d, i, n and s), and chitosan aligned fibers (e, j, o and t). Fibers substrates appear green due to material autofluorescence. Images were acquired at 60X magnification with different zoom. Scale bar: 40 μm. Percentages of cells with low, medium or high actin cytoskeleton organization ☐} standard error of the mean (SEM) 3 (u), 6 (v) and 24 (w) h after seeding are reported. Percentages of cells with low, medium or high numbers of focal adhesion points ☐} SEM 3 (x), 6 (y) and 24 (z) h after seeding are also reported. One-way ANOVA was used for statistical analysis. Asterisks denote statistically significant differences with *p ≤ 0.05, **p ≤ 0.01 and ***p ≤ 0.001 (Supplementary tables 11-16).

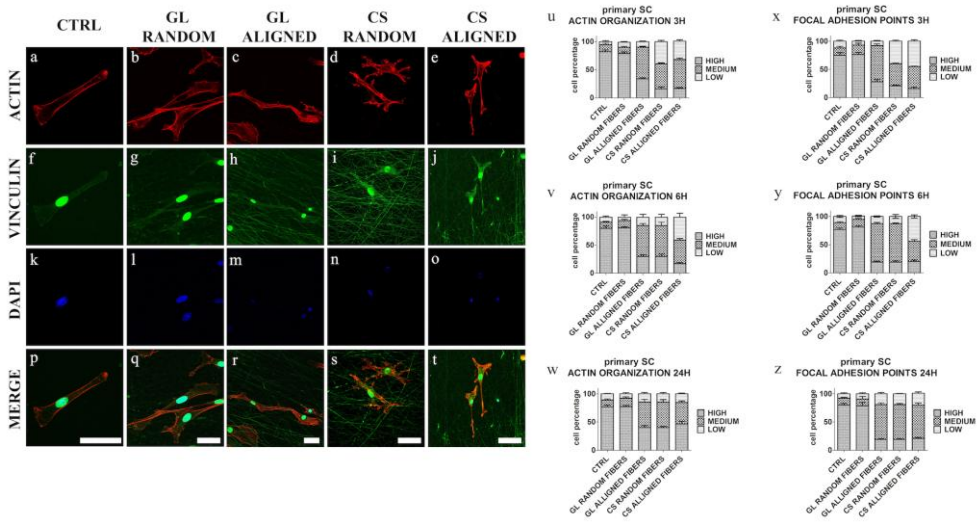

Figure 7. Primary SC actin cytoskeleton and focal adhesion points organization. Fluorescence images following phalloidin-actin (red), vinculin (green) and DAPI (blue) staining of SC on poly-l-lysine coated coverslips (control condition, a, f, k and p), gelatin random fibers (b, g, l and q), gelatin aligned fibers (c, h, m and r), chitosan random fibers (d, i, n and s), and chitosan aligned fibers (e, j, o and t). Fibers substrates appear green due to material autofluorescence. Images were acquired at 60X magnification with different zoom. Scale bar: 40 μm. Percentages of cells with low, medium or high actin cytoskeleton organization ☐} standard error of the mean (SEM) 3 (u), 6 (v) and 24 (w) h after seeding are reported. Percentages of cells with low, medium or high numbers of focal adhesion points ☐} SEM 3 (x), 6 (y) and 24 (z) h after seeding are also reported. One-way ANOVA was used for statistical analysis. Asterisks denote statistically significant differences with *$p \leq 0.05$, **$p \leq 0.01$ and ***$p \leq 0.001$ (Supplementary tables 17-22).

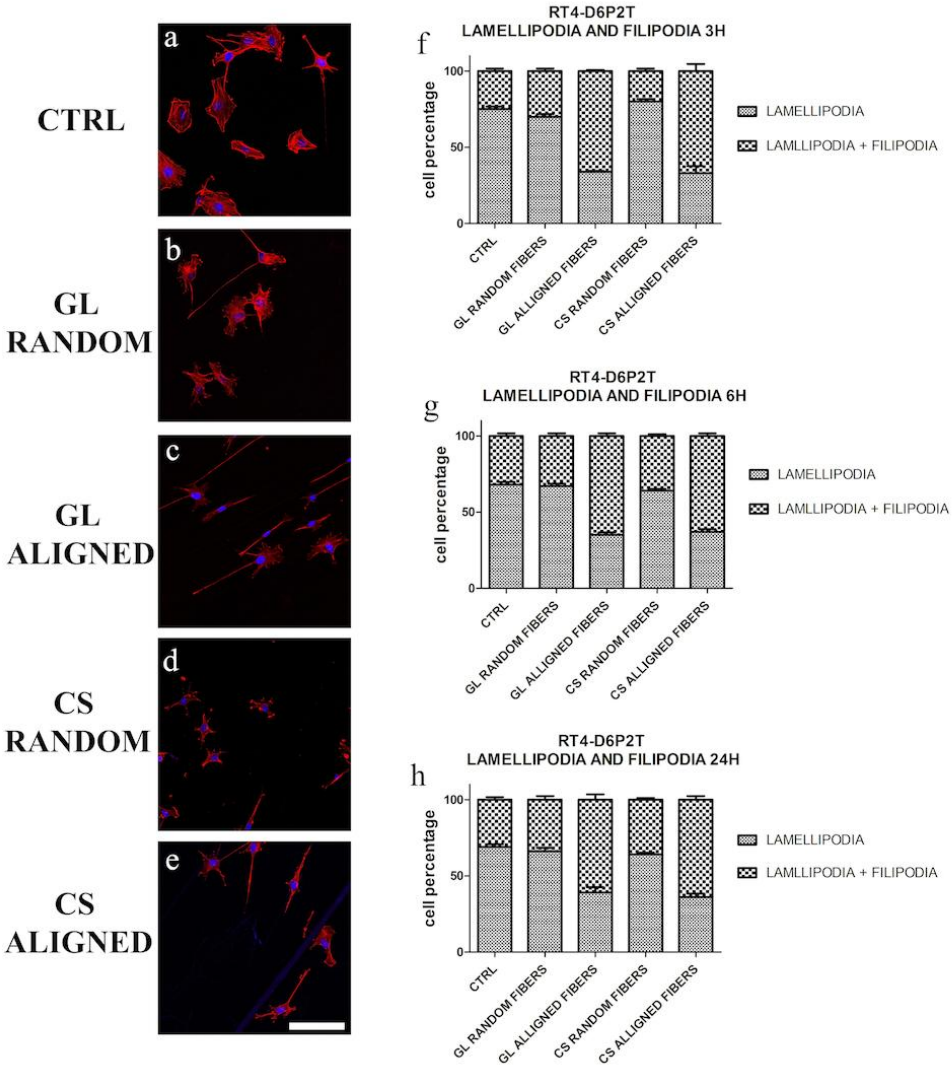

Figure 8. Lamellipodia and filopodia organization in RT4-D6P2T cells. Fluorescence images phalloidin (red) and DAPI (blue) staining of RT4-D6P2T cells seeded on poly-l-lysine coated coverslips (control condition, a), gelatin random fibers (b), gelatin aligned fibers (c), chitosan random fibers (d), and chitosan aligned fibers (e) 6 hours after seeding. Images were acquired at 40X magnification. Scale bar: 100 μm. Percentage of RT4-D6P2T cells characterized by lamellipodium and filopodia protrusions 3 (f), 6 (g) and 24 (h) h after seeding are expressed as mean ☐} standard error of the mean (SEM). One-way ANOVA was used for statistical analysis. Asterisks denote statistically significant differences with *p ≤ 0.05, **p ≤ 0.01 and ***p ≤ 0.001 (Supplementary tables 23-25).

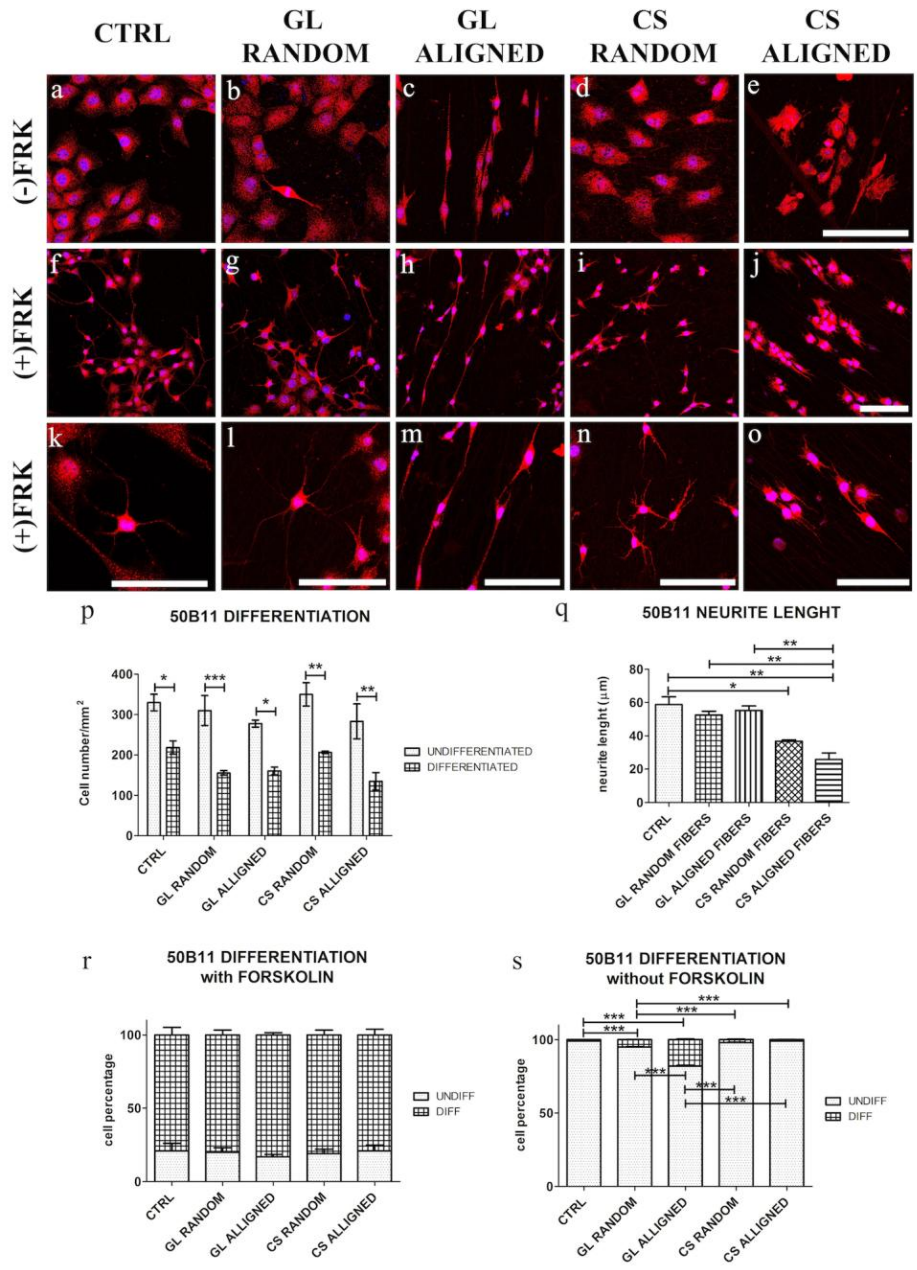

Figure 9. Lamellipodia and filopodia organization in primary SC. Fluorescence images phalloidin (red) and DAPI (blue) staining of SC seeded on poly-l-lysine coated coverslips (control condition, a), gelatin random fibers (b), gelatin aligned fibers (c), chitosan random fibers (d), and chitosan aligned fibers (e) 6 hours after seeding. Images were acquired at 40X magnification. Scale bar: 100 μm. Percentage of SC characterized by lamellipodium and filopodia protrusions 3 (f), 6 (g) and 24 (h) h after seeding are expressed as mean ☐} standard error of the mean (SEM). One-way ANOVA was used for statistical analysis. Asterisks denote statistically significant differences with *p ≤ 0.05, **p ≤ 0.01 and ***p ≤ 0.001 (Supplementary tables 26-28).

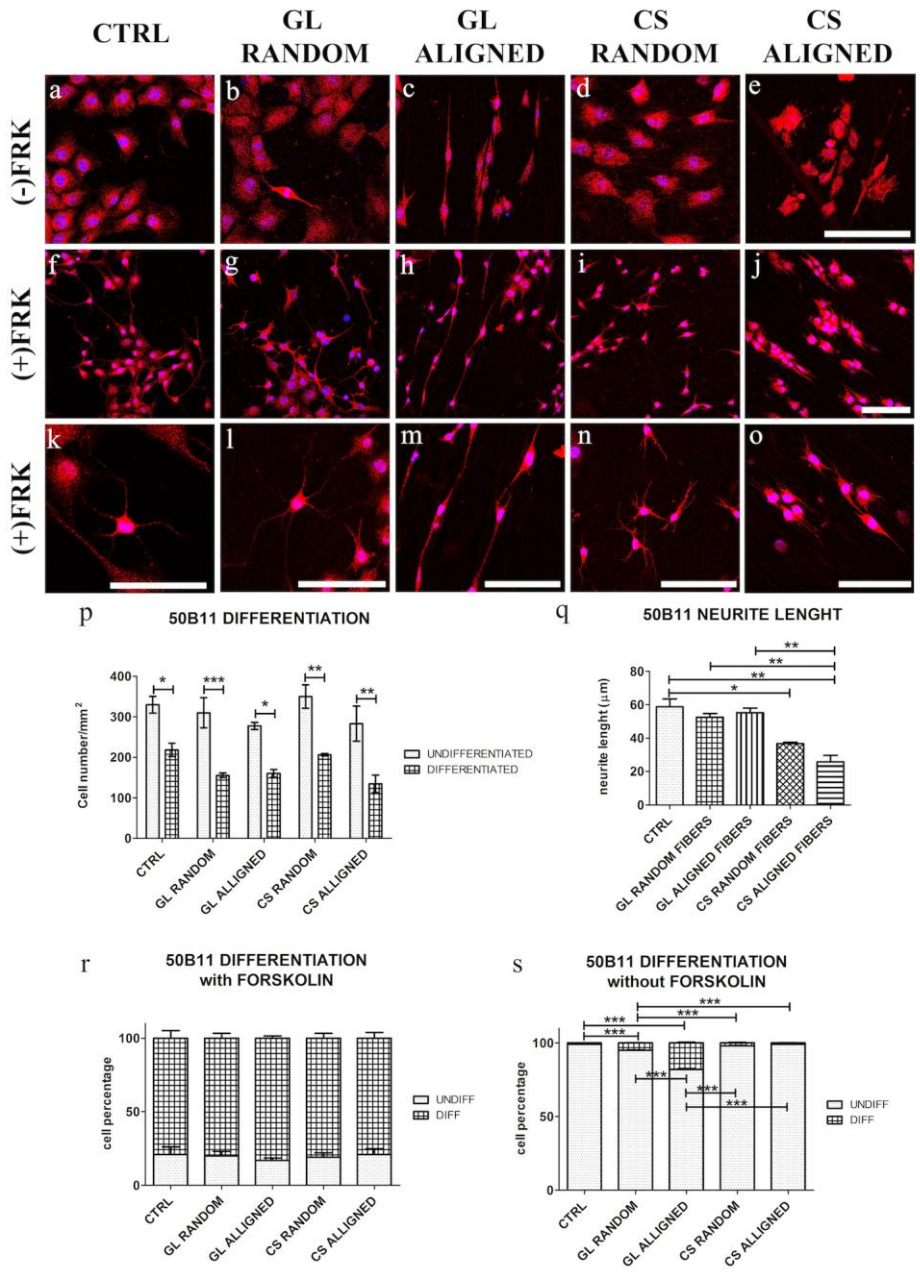

Figure 10. 50B11 cells differentiation. Confocal images after β-tubulin (red) and DAPI (blue) staining of B5011 cells seeded on poly-l-lysine coated coverslips (control condition, a, f, and k), random gelatin fibers (b, g, and l), aligned gelatin fibers (c, h and m), random chitosan fibers (d, i and n) and aligned chitosan fibers (e, j and o). 50B11 cells were cultured without (a-e) or with forskolin (f-o) addition to the culture medium. Images were acquired at 40X or 60X magnification with different zoom. Scale bar: 100 μm. 50B11 cell were counted and cell number is expressed as cells/mm2 ☐} standard error of the mean (SEM) (p); Neurite length is expressed as μm☐} SEM (q); 50B11 differentiated and undifferentiated cells in presence (r) or absence (s) of forskolin treatment are expressed as percentage of cells☐} SEM. One way ANOVA was used for statistical analysis. Asterisks reported in figure refer to significant statistical difference with * $p \leq 0.05$, ** $p \leq 0.01$ and *** $p \leq 0.001$. Two-way ANOVA was also used for statistical analysis. Asterisks refer to significant statistical difference with * $p \leq 0.05$, ** $p \leq 0.01$ and *** $p \leq 0.001$ (Supplementary tables 8-10).

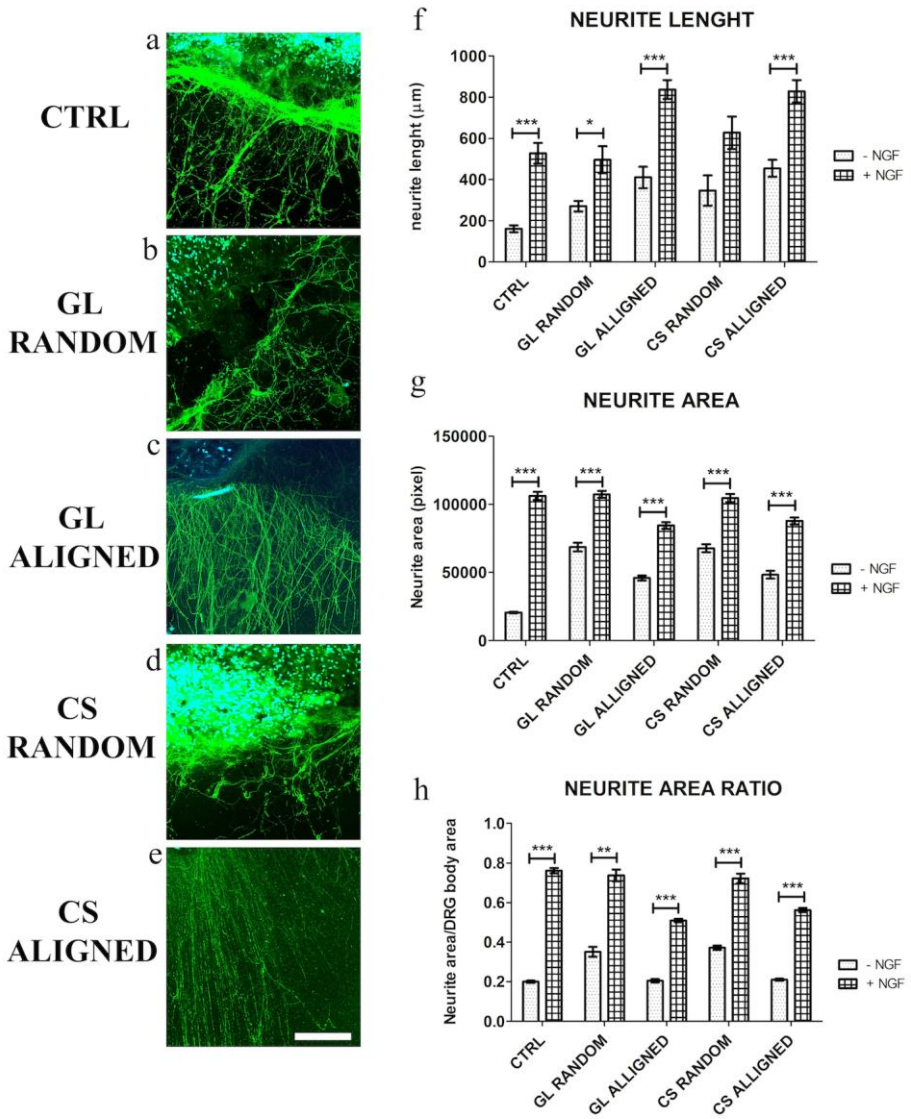

Figure 11. Fluorescence images after β-tubulin (green) and DAPI (blue) staining of DRG explants cultured on control condition (poly-l-lysine coated coverslips, a), random gelatin fibers (b), aligned gelatin fibers (c), random chitosan fibers (d) and aligned chitosan fibers (e) without (not shown) or with NGF (a-e). Images were acquired at 40X magnification. Scale bar: 100 µm. Axon length is expressed as µm ☐} standard error of the mean (SEM) (f), density as pixel ☐} SEM (g), sprouting area as DRG axon area/DRG axon area ratio ☐} SEM (h). One way ANOVA was used for statistical analysis. Asterisks reported in figure refer to significant statistical difference with * $p \leq 0.05$, ** $p \leq 0.01$ and *** $p \leq 0.001$. Two-way ANOVA was also used for statistical analysis. Asterisks refer to significant statistical difference with * $p \leq 0.05$, ** $p \leq 0.01$ and *** $p \leq 0.001$ (Supplementary tables 5-7).